Proposal of Single Sideband Modulation Scheme with Ideal Low Pass Filter for Wireless Communication Systems

Hiroaki Waraya and Masahiro Muraguchi
Department of Electrical Engineering, Tokyo University of Science
6-3-1 Niijuku, Katsushika-ku, Tokyo, 125-0051, Japan
E-mail: 4319583@ed.tus.ac.jp, murag@ee.kagu.tus.ac.jp

***Abstract* - Recently developed wireless communication systems primarily require a modulation scheme with higher spectral efficiency and higher quality. In this study, Single Sideband (SSB) modulation scheme that transmits two different signals at the same carrier frequency is proposed. Additionally, our proposed method employs a 4-times oversampled digital filter. The distance between the folded spectrum and the carrier frequency is quadrupled, and its filter creates a spectrum with a roll-off rate of zero on the transmission side. A digital filter with such characteristics can help reduce the burden of the subsequent analog filter. Under Additive White Gaussian Noise (AWGN) channel environment, Bit Error Rate (BER) performance of SSB quaternary Amplitude-Shift Keying (4ASK) at roll-off rate of zero is superior by 3 dB with respect to Carrier-to-Noise Ratio (CNR) to 16 Quadrature Amplitude Modulation (16QAM) of the same spectral efficiency, without affecting the effect of extra Hilbert components.**

Keywords - SSB; Hilbert Transform; Multiplexing; Digital Filter; Roll-off Rate.

I. INTRODUCTION

Recently, the demand for wireless communication systems has been increasing with the spread of smartphones, digital terrestrial broadcastings, and wireless Local Area Network (LANs). The frequency resources are being depleted in Ultra High Frequency (UHF) and Super High Frequency (SHF) bands utilized by many wireless systems. So, the high-priority issue for the subsequent wireless systems is a revolutionary modulation scheme with higher spectral efficiency and higher quality. This study proposes SSB modulation scheme with an ideal digital filter to improve the quality of wireless systems.

The SSB system sends data at half the occupied bandwidth when compared to that of the Double Sideband (DSB) system. The SSB signal can be produced by combining the Hilbert transform and quadrature multiplexing, which causes in-phase addition of one sideband and cancellation of the opposite sideband. However, the SSB system is only effective in scalar modulation, such as ASK modulation [1]. In contrast, quadrature modulation, which is a typical DSB modulation, employs two carrier waves of the same frequency that are out of phase with each other by 90°. When the SSB modulation is incorporated with quadrature modulation, the spectrum efficiency is expected to be twice as high as conventional scheme.

Unfortunately, they are not independent of each other as both modulations use the same signal processing for quadrature multiplexing. The in-phase component comprises the I-data and Hilbert transform of Q-data, and the quadrature component comprises Q-data and Hilbert transform of I-data on the receiver side. Thus, lossless demodulation cannot be performed analytically because of extra Hilbert components. In fact, several researchers have recently investigated the SSB Quadrature Phase-Shift Keying (QPSK) modulation scheme. For example, several researches successfully transmitted not only SSB QPSK but also SSB Multivalued Quadrature Amplitude Modulation (M-QAM), using turbo equalization on the receiver side [2]-[5]. However, there are drawbacks that the occupied bandwidth is increased due to the addition of the error correction code, and that their proposed SSB QPSK is sensitive to the residual phase-error under the fading channel because of the effect of extra Hilbert components.

In this study, a single-carrier transmission of SSB 4ASK modulation scheme is proposed. It transmits different signals in Upper Sideband (USB) and Lower Sideband (LSB) without extra Hilbert components, at the same carrier frequency. Under AWGN channel environment, BER performance of the proposed scheme is superior by 3 dB in terms of CNR to the same data rate and the same occupied bandwidth of 16QAM signal. Additionally, the proposed SSB modulation scheme also maintains the good performance in higher order modulation.

In contrast, our proposed scheme employs a 4-times oversampled digital filter to obtain an ideal spectrum. When SSB modulation is applied to a QPSK with a raised cosine filter, a drawback is that the BER performance at low roll-off rate deteriorates even in AWGN channel environment because of extra Hilbert components [6]. However, the proposed digital filter with oversampling produces the ideal Low Pass Filter (LPF) with a roll-off rate of zero, and the BER performance does not change when the digital filter is applied. Additionally, the burden of a subsequent analog filter can be reduced on the transmission side, because the alias can be moved to a position that is four times farther away by oversampling.

The remainder of this paper is organized into as follows: Section II explains about related works. Section III explains how the SSB modulation is performed, and Section IV gives details on digital LPF. Section V presents our proposed SSB

4PAM modulation scheme using digital LPF and describes how two different data on the same carrier frequency are multiplexed. Section VI presents the performance evaluation and simulation results of the proposed scheme. Finally, the concluding remarks of the study are mentioned in Section VII.

II. Related Works

In the field of wireless communication, several studies have conducted to apply SSB modulation, which is a scalar modulation, to a quadrature amplitude modulation such as QPSK. This modulation method is called the Quadrature-Single Sideband (Q-SSB) modulation. The Q-SSB modulation scheme is expected to have twice the spectral efficiency. The time-domain signal of the conventional Q-SSB modulation scheme in the case of USB is expressed as follows:

$$S_u(t) = \{I_u(t) + \widehat{Q_u}(t)\} cos\, 2\pi f_c t + \{-\widehat{I_u}(t) + Q_u(t)\} sin\, 2\pi f_c t. \quad (1)$$

On the receiver side, $\{I_u(t) + \widehat{Q_u}(t)\}$ is extracted in the in-phase component, and $\{-\widehat{I_u}(t) + Q_u(t)\}$ is extracted in the quadrature component. For example, Fig. 1 depicts the receiving signal $\{I_u(t) + \widehat{Q_u}(t)\}$ in the time domain. However, the BER performance deteriorates significantly, because extra Hilbert components, i.e., $\widehat{Q_u}(t)$ and $-\widehat{I_u}(t)$, cannot be removed analytically. In a previous research, a turbo equalizer was employed on the receiver side to suppress the degradation of BER performance. In this case, while the received signal with extra Hilbert components is corrected by the equalizer, the bandwidth is increased owing to the addition of the error correction code and it is sensitive to the residual phase-error under the fading channel. On the other hand, $Q_u(t)$ can be extracted via detection of the peak value of Hilbert component as depicted in Fig. 1. However, the BER performance cannot be improved adequately without an error correction code. In this way, when introducing Q-SSB modulation scheme, how to solve the problem of extra Hilbert components is the important issue [2]-[5].

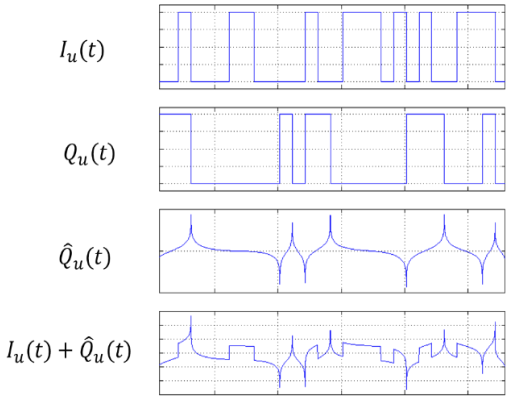

Figure 1. Receiving signal of $\{I_u(t) + \widehat{Q_u}(t)\}$

On the other hand, when considering a practical Q-SSB modulation scheme with the raised cosine filter at low roll-off rate, the aperture ratio of the eye pattern becomes low due to the presence of extra Hilbert components. Therefore, the BER performance deteriorate as the roll-off rate decreases in not only the fading channel but also AWGN channel, even if turbo equalizer is implemented [6].

As can be seen from the related works described above, the main issues in the Q-SSB modulation scheme are to remove extra Hilbert components and to form a practical spectrum with a roll-off rate of zero without the penalty of BER performance.

III. SSB Modulation

In this section, the performance of the SSB modulation is presented, and the characteristics of SSB modulation and Hilbert transform are explained.

A. Characteristics of SSB modulation

Amplitude modulation (AM) is a technique that multiplies the carrier wave with the information signal and changes the amplitude of the transmission signal in direct proportion to the size of the information signal. The transmission signal $S(t)$ in a general AM method can be represented as follows:

$$S(t) = A[1 + k \cdot m(t)] \cdot cos(2\pi f_c t + \varphi), \quad (2)$$

where, A is the signal amplitude, k is the modulation index $(0 \le k \le 1)$, f_c is the carrier frequency, and φ is the carrier phase. A general envelope waveform of the AM method has an $m(t)$ waveform centered around $\pm A$, the amplitude. If $m(t) = cos\, 2\pi f_m t$, (2) can be rewritten as follows:

$$\begin{aligned} S(t) &= A(1 + cos 2\pi f_m t) \cdot cos\, 2\pi f_c t \\ &= A\, cos\, 2\pi f_c t + \frac{A}{2} cos\, 2\pi (f_c - f_m) t \\ &\quad + \frac{A}{2} cos\, 2\pi (f_c + f_m) t. \end{aligned} \quad (3)$$

For simplifying (3), $A = 1, k = 1$, and $\varphi = 0$. In (3), the first term represents the carrier wave component. The second and third terms are components of the information signal $m(t)$. The lower frequency component than the carrier wave, in the second term, constitutes the Lower Sideband (LSB); and the higher frequency component than the carrier wave, in the third term, constitutes the Upper Sideband (USB). Fig. 2 depicts the spectrum of DSB modulation.

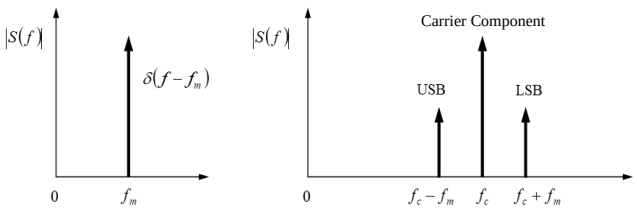

Figure 2. Spectrum of DSB modulation

As depicted in Fig. 2, a spectrum is generated at a location separated by $\pm f_m$ from the carrier frequency f_c. Thus, DSB modulation is a method of transferring an information signal to a carrier band and communicating utilizing the LSB and USB. As observed from (3), the transmission of information is possible either by utilizing the LSB or USB, as they both contain the same information. The transmission of information utilizing only one sideband is called SSB modulation method.

Fig. 3 depicts the SSB transmission spectrum obtained by utilizing the LSB. Here, the negative frequency region is shown as an arithmetic expression, but only the positive frequency region appears as a real signal. In comparison to features of the DSB method, the most prominent feature of the SSB method is that the occupied bandwidth frequency is halved.

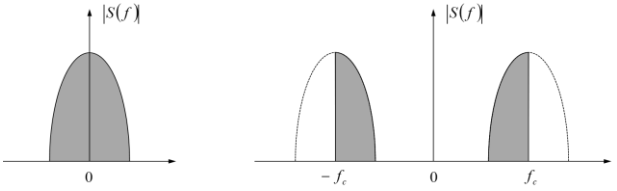

(a) Base band signal (b) SSB signal

Figure 3. SSB transmission spectrum using LSB

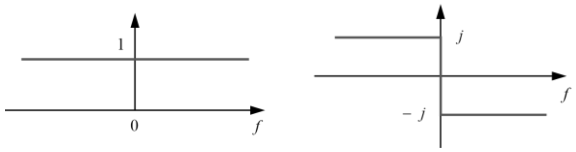

(a) Amplitude characteristic (b) Phase characteristic

Figure 4. Hilbert transform characteristics

B. Hilbert transform

The phase shift method is a way of generating an SSB signal using two 90° phase shifters. The Hilbert transform of a signal $\hat{x}(t)$ is defined as the transform in which the phase angle of all components of the signal is shifted 90° [7]-[8]. It is represented as follows:

$$\hat{x}(t) = H[x(t)] = \frac{1}{\pi}\int_{-\infty}^{\infty}\frac{x(\tau)}{t-\tau}d\tau = x(t) * \frac{1}{\pi t}. \qquad (4)$$

Here, the signum function is represented as

$$sgn(t) = \begin{Bmatrix} 1, & t > 0 \\ -1, & t < 0 \end{Bmatrix} \Leftrightarrow \frac{1}{j\pi f}. \qquad (5)$$

The value of this function in the positive time domain is 1, and in the negative time domain it is -1. On application of the duality theorem to (5), the frequency response of the Hilbert transform $H(\omega)$ is represented as follows:

$$\frac{1}{\pi t} = h(t) \Leftrightarrow H(\omega) = -jsgn(\omega) = \begin{cases} -j, & \omega > 0 \\ j, & \omega < 0. \end{cases} \qquad (6)$$

From (4) and (6), and on application of the convolution in the time domain to the Hilbert transform, the frequency response of the signal transformed by the Hilbert transform is represented as follows:

$$\hat{x}(t) = x(t) * \frac{1}{\pi t} \Leftrightarrow \hat{X}(\omega) = X(\omega)\cdot(-j\,sgn(\omega)). \qquad (7)$$

As indicated in (6) and (7), the Hilbert transform delays by 90° at positive frequencies and advances 90° at negative frequencies in the frequency domain. Additionally, the amplitude characteristic is constant regardless of the frequency. Fig. 4 depicts the characteristics of the Hilbert transform.

The following explains the repeatability of the Hilbert transform. When the Hilbert transform is repeated on the signal that has been processed using the Hilbert transform, the equation is represented as follows:

$$\begin{aligned} \hat{\hat{X}}(\omega) &= \{-j\,sgn(\omega)\} \times \{-j\,sgn(\omega)\cdot X(\omega)\} \\ &= -X(\omega), \end{aligned} \qquad (8)$$

and the inverted original signal is the output. In contrast, if it is a linear transform, the equation is represented as follows:

$$\begin{aligned} H[m(t) \pm n(t)] &= \frac{1}{\pi}\int_{-\infty}^{\infty}\frac{m(\tau) \pm n(\tau)}{t-\tau}d\tau \\ &= H[m(t)] \pm H[n(t)]. \end{aligned} \qquad (9)$$

Fig. 5 depicts the spectrum transition of the SSB modulation [9]-[10]. In Fig. 5, $S_{USB}(t)$ *and* $S_{LSB}(t)$ of the transmitted signal on the frequency domain is represented as follows:

$$S(f) = S_I(f) \pm S_Q(f) = M(f) \pm sgn(f)M(f), \qquad (10)$$

where, $M(f)$ is the modulation signal and $sgn(f)M(f)$ is the Hilbert transform of $M(f)$. In (10) and Fig. 5, when $S_I(f)$ and $S_Q(f)$ are added, SSB modulation by LSB is performed; on the contrary, when they are subtracted, SSB modulation by USB is performed.

On the receiver side, $M(f)$ is extracted at the in-phase component and $\widehat{M}(f)$ is extracted at the quadrature component, as depicted in Fig. 5. As observed from (8), the same signal as the in-phase component can be obtained at the quadrature component upon performing Hilbert transform again. Then, the in-phase and the quadrature components are added to the receiver side.

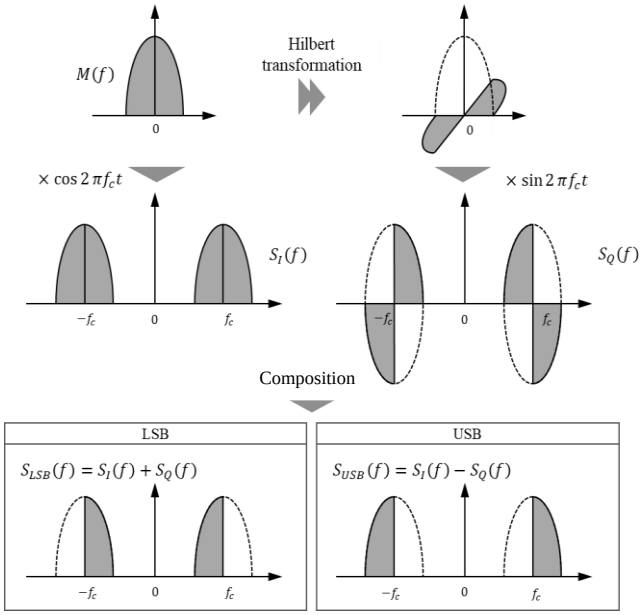

Figure 5. Generating SSB modulation signal

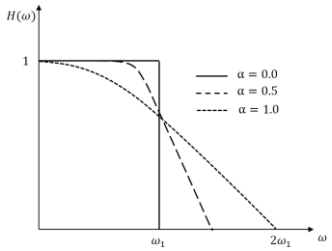

Figure 6. Frequency response of the raised cosine filter

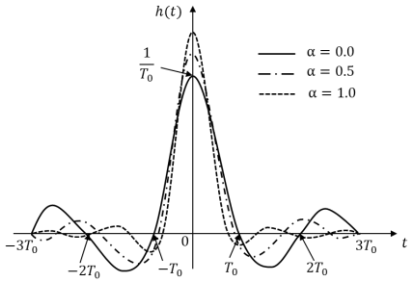

Figure 7. Impulse response of the raised cosine filter

A modulation scheme with such a demodulation scheme is called a Dual Branch SSB (DB-SSB) modulation scheme [11], and it is advantageous in that BER performance is improved by 3 dB. In the DB-SSB demodulation circuit, the variance σ^2 is doubled and the average amplitude E_b of the signal is also doubled in AWGN channel environment by adding the in-phase and quadrature components. Therefore, it can be observed that $|E_b|^2/|\sigma|^2$ of the DB-SSB scheme is superior by 3 dB.

IV. DIGITAL FILTER

In this section, the optimal transmission filter design of its modulation scheme is explained.

A. Analog LPF filter

As one of our purposes of this study is to improve the frequency efficiency, the extra occupied bandwidth should be compressed as much as possible. Typically, a spectrum shaping is performed through LPF to prevent the emission of unnecessary radio waves outside the transmission band. The characteristic of a cosine roll-off filter is often considered as a representative of the LPF. The frequency response of the raised cosine filter is represented as follows:

$$H(\omega) = \begin{cases} \sqrt{\frac{1}{2}\left[1 - \sin\left\{\frac{\pi|\omega| - \omega_1}{2\alpha\omega_1}\right\}\right]}, & (1-\alpha)\omega_1 \le |\omega| \le (1+\alpha)\omega_1 \\ 1, & |\omega| \le (1-\alpha)\omega_1 \\ 0, & |\omega| \ge (1+\alpha)\omega_1 \end{cases} \quad (11)$$

where, ω_1 is equal to π/T_0. Normally, the Nyquist interval is set identical to the symbol interval. Fig. 6 depicts the frequency response of the raised cosine filter when the roll-off rate is changed. Fig. 7 depicts the impulse response of the raised cosine filter.

As observed from Fig. 6, the transmission bandwidth becomes wider as α increases, and the bandwidth doubles when $\alpha = 1$.

The impulse response of the raised cosine filter is represented via an Inverse Fast Fourier Transform (IFFT) being performed on the frequency response. The equation thereof is represented as follows:

$$h(t) = \frac{1}{2\pi}\int_{-\infty}^{\infty} H(\omega)e^{j\omega t}d\omega$$

$$= \frac{1}{1 - 16\frac{\alpha^2 t^2}{T_0^2}}\left[\frac{\sin\left\{(1-\alpha)\frac{\pi t}{T_0}\right\}}{\frac{\pi t}{T_0}} + \frac{4\alpha}{\pi}\cos\left\{(1+\alpha)\frac{\pi t}{T_0}\right\}\right]. \quad (12)$$

As observed from Fig. 7, the vibration of the impulse response is large, and its response converges slowly, in the case of a steep LPF (α = 0). In contrast, when α is increased, the vibration of the impulse response is small, and its response converges quickly.

If the raised cosine filter, which is a steep LPF (α = 0), is used to improve the frequency efficiency, the side lobe of the impulse response increases and the aperture ratio of the eye pattern decreases. In such cases, the sampling cannot be performed adequately. There is a tradeoff between the amplitude characteristic of the passband and the blocking region of the LPF. Therefore, it is theoretically difficult to completely remove the out-of-band radiation using an analog LPF.

B. Digital Filter with oversampling

As it is difficult to demodulate the receiving signal, in the case of the analog filter of an ideal LPF, the spectrum of the proposed scheme is shaped via digital filter processing. The

digital filter with oversampling produces the ideal LPF, with a roll-off rate of zero. Fig. 8 depicts the configuration around the digital filter with oversampling. After the information signal is mapped, a Fast Fourier Transform (FFT) is performed to spread the signal in the frequency domain. The signal on the frequency domain by the FFT is represented as follows:

$$F(k) = \frac{1}{\sqrt{N}} \sum_{t=0}^{N-1} f(t) \cdot e^{-\frac{j2\pi kt}{N}}. \ (k = 0,1, \dots, N-1) \quad (13)$$

where, $F(k)$ is the frequency-domain signal, and $f(t)$ is the time-domain signal. Then, nulls that are three times FFT length, N, are inserted into the information signal in the frequency domain. As depicted in Fig. 8, the 3N-nulls are inserted, in the middle of the symbol, so that the LSB data and USB data are at both ends of the symbol. Such a processing method is called oversampling. The spectrum thereof is represented in Fig. 9. As observed from Fig. 9, the bandwidth can be compressed to half the original frequency bandwidth. As a result, the spectrum of the signal obtained from the digital filter is in the form of a roll-off rate of zero. Additionally, the alias can be kept sufficiently away from the main lobe, which facilitates subsequent LPF that attenuates the folded spectrum.

The process of inserting 3N-nulls is equivalent to multiplying a rectangular wave in the frequency domain, as depicted in Fig. 9. The signal on the frequency domain after oversampling is represented as follows:

$$F_R(f) = F(f) \cdot rect(f), \quad (14)$$

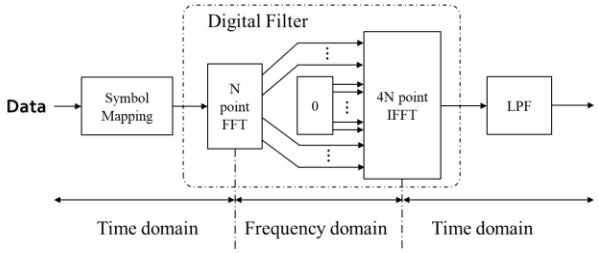

Figure 8. Configuration of the oversampled digital filter

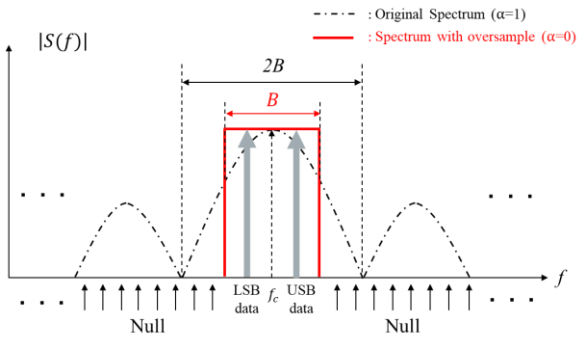

Figure 9. Spectrum with the digital filter

where,

$$rect(f) = \begin{cases} 0, & N < |f| \le 4N \\ 1, & |f| \le N \end{cases}. \quad (15)$$

The inverse Fourier transform of (15) is represented as

$$\int_{-N}^{N} rect(f) \cdot e^{j2\pi ft} dt = \frac{1}{\pi t} sin\left(\frac{\pi t}{T}\right), \quad (16)$$

where, N=$1/2T$, and T is the sampling interval. If $f_R(t)$ is the inverse Fourier transform of $F_R(f)$, then

$$\begin{aligned} f_R(t) &= f(t) * \frac{1}{\pi t} sin\left(\frac{\pi t}{T}\right) \\ &= \int_{-\infty}^{\infty} f(t') \frac{1}{\pi(t-t')} sin\left\{\frac{\pi(t-t')}{T}\right\} dt'. \end{aligned} \quad (17)$$

As $f_R(t)$ is the discrete signal, $t' = nT$. Then,

$$f_R(t) = \sum_{n=-\infty}^{\infty} f(nT) \frac{1}{\pi(t-nT)} sin\left\{\frac{\pi(t-nT)}{T}\right\}. \quad (18)$$

where $t = kT/4$; IFFT size increases to 4N, which is four-times the oversampled size. As indicated in (18), the time-domain signal after the digital filter processing is represented by the sum of the *sinc* function. Then, the signal that is interpolated between the original signals is generated.

Fig. 10 depicts the time-domain signal after the digital filter processing. The red waveform is the signal before the digital filter processing, and the blue waveform is the signal after the digital filter processing. As depicted in Fig. 10, the oversampling interpolates the part of the transient response between the original signal points, i.e., the quadrupled oversampling interpolates three points between two signal points.

Fig. 11 (a) depicts the eye pattern of an analog steep LPF and Fig. 11(b) depicts the eye pattern, when an LPF is performed after the digital filter processing.

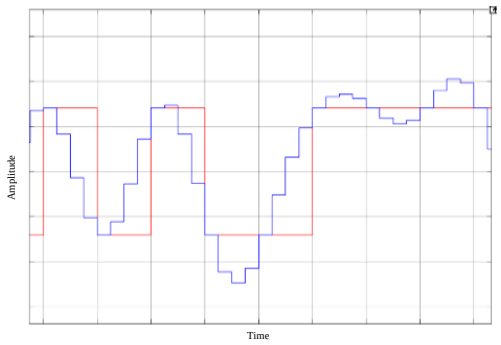

Figure 10. Time domain signal after the digital filter

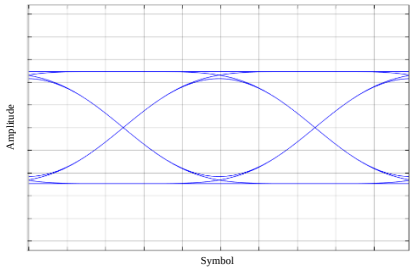

(a) Analog steep filter

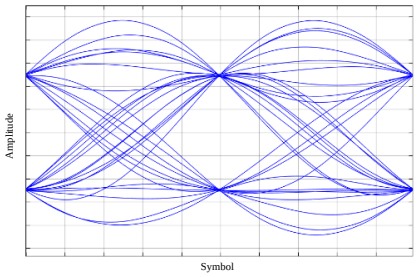

(b) Digital filter

Figure 11. Eye pattern of the signal with each steep filter

It can be seen that the aperture ratio of the eye pattern does not decrease when the digital filter is applied, while the aperture ratio of an analog steep filter, depicted in Fig. 11 (a), decreases.

V. PROPOSED METHOD

In this section, the proposed method that uses the SSB modulation is presented, and how two different data of the same frequency are multiplexed is described.

A. The proposed method

As a new modulation scheme, a method that adds two data with different amplitudes of the same component is proposed in [1]. The time-domain signal of the SSB method, in the case of USB is expressed as follows:

$$S_u(t) = \left\{I_u(t) + \frac{1}{2}Q_u(t)\right\} cos\ 2\pi f_c t + \left\{-\widehat{I_u}(t) - \frac{1}{2}\widehat{Q_u}(t)\right\} sin\ 2\pi f_c t. \quad (19)$$

Fig. 12 depicts the amplitude characteristic of the Q-SSB expressed in (19). Through this method, the I-data and Q-data are extracted on the in-phase component, and Hilbert components of the I-data and Q-data are extracted on the quadrature component. This method is similar to the DB-SSB modulation scheme described in Section III. The BER performance is improved by 3 dB. Regarding the method of separating the I-data and Q-data, the I-data is first obtained by determining whether the value is positive or negative with zero as a threshold value; and the Q-data is obtained by subtracting the I-data from the original signal.

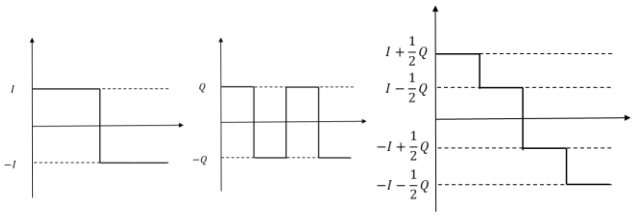

Figure 12. Amplitude of the Q-SSB signal, as in (19)

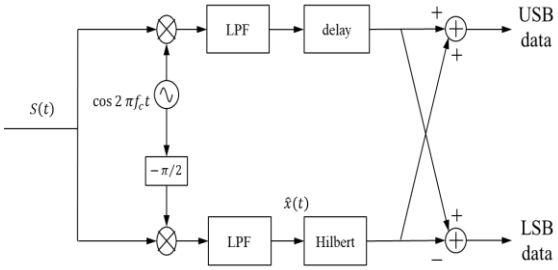

Figure 13. Multiplexed SSB demodulation circuit

However, the signal depicted in Fig. 12 is equivalent to the 4ASK modulation scheme, which increases the amplitude modulation order. Therefore, the 4PAM-based SSB modulation scheme is proposed in this study.

In contrast, our proposed scheme utilizes the digital filter, described in Section IV, which creates a spectrum with a roll-off rate of zero. The burden of the analog filter after the digital filter processing can be reduced on the transmission side.

B. Multiplexing SSB modulation method

In the proposed scheme, different information on LSB and USB is transmitted at the same carrier frequency. From (10), the signal generated by multiplexing different information on USB and LSB is represented as follows:

$$S(t) = \{m_u(t) + m_l(t)\} cos\ 2\pi f_c t + \{-\widehat{m_u}(t) + \widehat{m_l}(t)\} sin\ 2\pi f_c t, \quad (20)$$

where, $m_u(t)$ is the signal on USB and $m_l(t)$ is the signal on LSB. Fig. 13 depicts the demodulation circuit for the multiplexed SSB signal. In the upper portion of Fig. 13, $S(t)$ from (20) is multiplied by $cos\ 2\pi f_c t$, and passed through the LPF. This signal is represented as in (21). In the lower portion of Fig. 13, $S(t)$ from (20) is multiplied by $sin\ 2\pi f_c t$, passed through the LPF, and transformed by the Hilbert transform. That signal is represented as in (22).

$$S_{cos}(t) = m_u(t) + m_l(t) \quad (21)$$

$$\hat{S}_{sin}(t) = m_u(t) - m_l(t) \quad (22)$$

Thus, the USB signal is extracted by adding (21) and (22), and the LSB signal is extracted by subtracting (21) from (22).

VI. PERFORMANCE EVALUATION BY SIMULATION

In this study, the spectrum and BER performances of the 4ASK based SSB signal with a digital filter are confirmed. Under the AWGN channel environment, the BER performance of the proposed scheme is superior by 3 dB in the CNR, where compared to the same data rate and the same occupied bandwidth of the 16QAM signal. For accurately analyzing the BER performance of the SSB modulation scheme, the BER performance was measured using E_b/N_0 and CNR. E_b/N_0 is calculated by;

$$E_b/N_0 = CNR + 10log_{10}\left(\frac{T_{sym}}{2T_{samp}}\right) - 10log_{10}(k), \quad (23)$$

where, T_{sym} is the symbol period, T_{samp} is the sample period, and k is the number of information bits per symbol.

A. Simulation specification

A simulation using MATLAB/Simulink was performed for our proposed method. Table I illustrates the simulation specifications used in this research.

TABLE I. SIMULATION SPECIFICATION.

Parameter	Proposed system	Comparison system
Primary Modulation	4PAM, 8PAM, 16PAM	16QAM, 64QAM, 256QAM
Secondary Modulation	SSB Modulation	Quadrature Modulation
FFT Size	64	64
IFFT Size	256	256
Data Rate	2×2Mbps	4Mbps
Carrier Frequency	40 MHz	40 MHz
Data Size	Single Carrier	Single Carrier
Channel Model	AWGN	AWGN

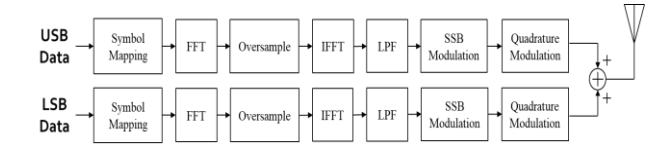

(a) Transmission Side

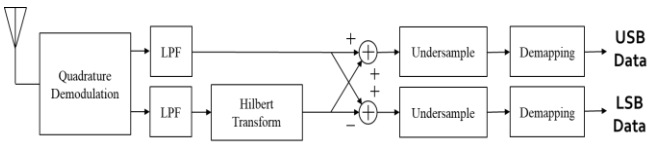

(b) Receiver Side

Figure 14. Block diagram of the proposed system

As illustrated in Table I, the 4 Pulse-Amplitude Modulation (4PAM) based SSB modulation is compared with the 16QAM for equivalent bandwidths. Similarly, the PAM-based SSB modulation is compared with the 64QAM and 256QAM to confirm that the advantage of SSB modulation can be utilized even when the proposed scheme is high-ordered. Fig. 14 depicts a block diagram of the proposed system. The undersample on the receiver side extracts data only at appropriate points of the time-domain signal, as depicted in Fig. 10.

B. Simulation results

Fig. 15 depicts the spectrum of the Q-SSB signal that transmits data only at the LSB. Fig. 16 depicts the BER performance in the CNR of the proposed method. Fig. 17 depicts the BER performance in the E_b/N_0 of the proposed method.

As observed from Fig. 15, a part of the opposite sideband is suppressed by the Hilbert transform. It expresses that the Q-SSB signal can be transmitted using only the LSB. As observed from Fig. 16, the SSB method has a BER performance in CNR of 3 dB superior than the DSB 16QAM scheme, which has the same occupied bandwidth. Simultaneously, Fig. 17 depicts that the BER performance of the SSB method, E_b/N_0, is equivalent to that of the DSB 16QAM scheme that has the same spectral efficiency.

Therefore, it is confirmed from Fig. 16 and Fig. 17 that the BER performance of the Q-SSB modulation scheme is superior by 3 dB to that of the 16QAM scheme, depending on the size of the information bit number, k, according to (23). The conventional 4PAM scheme requires only a cosine wave when performing the up-conversion, but the SSB 4PAM scheme also requires a sine wave. Therefore, the signal power of the proposed method on the transmission side is twice as large as that of the conventional 4PAM scheme. This means that the E_b/N_0 of the proposed method deteriorates by 3 dB. However, the proposed method can improve the E_b/N_0 by 3 dB, by implementing the DB-SSB modulation scheme on the receiver side. As mentioned in Section III, the variance σ^2 of AWGN is doubled and the signal average amplitude E_b is also doubled in the demodulation circuit of DB-SSB, by adding in-phase and quadrature components. As a result, the BER performance in $|E_b|^2/|\sigma|^2$ of the proposed scheme is the same as that of the 16QAM scheme with equivalent occupied bandwidth. In terms of BER performance in CNR, the proposed scheme, which is a 2-bit transmission, is 3 dB superior than the 16QAM scheme, which is a 4-bit transmission, from the viewpoint of the number of information bits, k. Such advantages can only be obtained by the discrete signal processing.

Fig. 18 depicts the BER performance in CNR for the 8PAM-based SSB modulation scheme and 16PAM-based SSB modulation scheme. The BER performance of SSB 8PAM is 3 dB superior than that of the DSB 64QAM, which has the same occupied bandwidth. The same is true when comparing 16PAM and 256QAM.

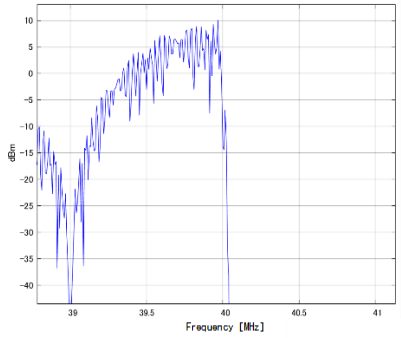

Figure 15. Spectrum of the Q-SSB system

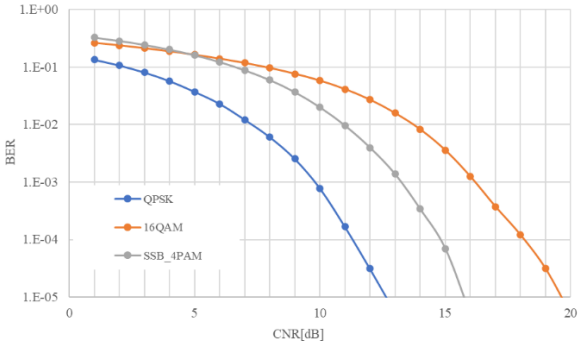

Figure 16. BER performance in the CNR of SSB 4PAM scheme

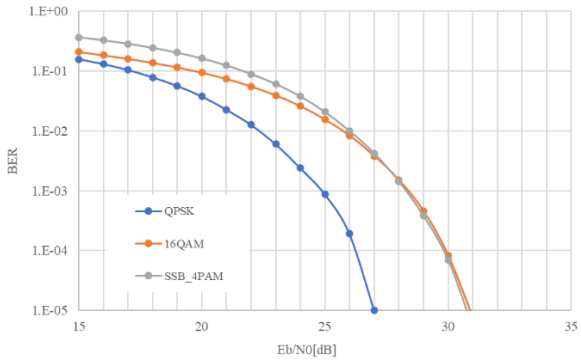

Figure 17. BER performance in the E_b/N_0 of the proposed scheme

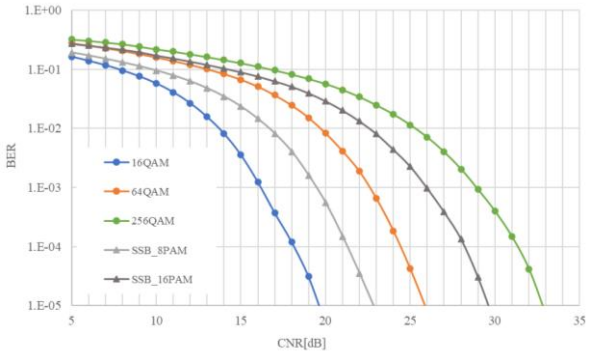

Figure 18. BER performance of SSB 8PAM and SSB 16PAM

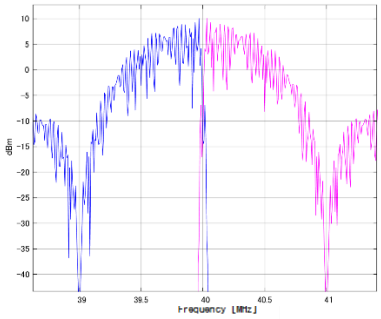

Figure 19. Spectrum of multiplexing SSB modulation scheme

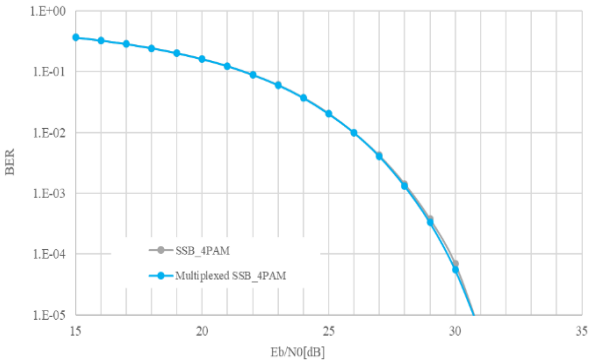

Figure 20. BER performance of multiplexed SSB modulation scheme

From Fig. 16 and Fig. 18, it can be confirmed that the proposed SSB modulation scheme maintains the good performance in higher order modulation, in the AWGN channel environment.

Fig. 19 depicts the spectrum of the multiplexed Q-SSB signal. Fig. 20 compares the BER performance of the Q-SSB signal with data only on the USB and BER performance of the multiplexed SSB modulation scheme. As observed from Fig. 19, each sideband part suppresses the opposite sideband by the Hilbert transform, so that two different 4PAM transmissions can be performed simultaneously on the USB and LSB. In Fig. 20, the multiplexed SSB modulation scheme has the BER performance in E_b/N_0 equivalent to the SSB modulation scheme that transmits data on only USB or LSB.

The reason why the BER performance does not change even when two signals are multiplexed is that the frequency bandwidth doubles as the number of information bits changes from 2-bit to 4-bit, although the signal power that is added to the signal of the USB and LSB bands doubles on the transmission side at the same time.

Fig. 21 depicts the spectrum of the multiplexed SSB modulation scheme with the digital filter compared to that of the 16QAM modulation scheme. Fig. 22 depicts the folded spectrum of the proposed scheme with a digital filter. Fig. 23 depicts the BER performance of the multiplexed SSB modulation scheme with a digital filter compared to that of the multiplexed SSB modulation scheme without a digital filter.

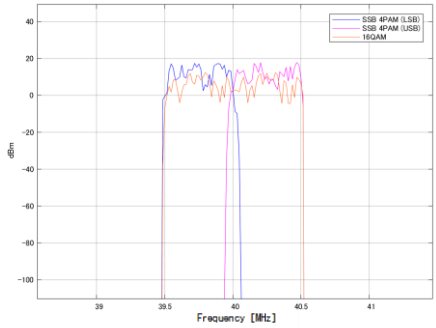

Figure 21. Spectrum of the SSB scheme with the digital filter

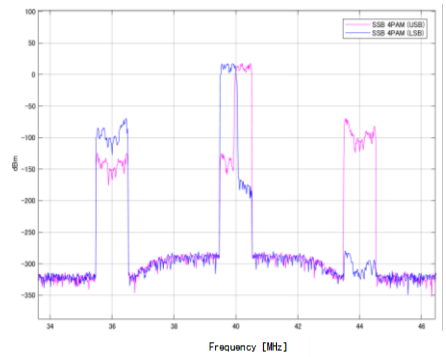

Figure 22. Folded spectrum of the proposed scheme with the digital filter

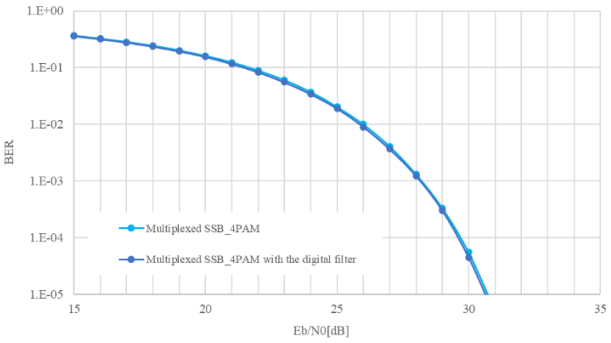

Figure 23. BER performance of the SSB scheme with the digital filter

As observed from Fig. 21, two different SSB 4PAM signals are transmitted adjacent to each other, after a sharp filter processing with a roll-off rate of zero. As a result, the proposed scheme realizes the ideal spectrum on the transmission side with the minimum required bandwidth because the SSB modulation removes the extra band on one side and the digital filter halves the occupied band. The spectral efficiency of the proposed method is equivalent to that of the comparison method, and it is confirmed that it can take advantage of the BER performance without lowering the spectral efficiency.

The frequency of the folded spectrum is 4MHz apart from the carrier frequency of the main lobe when the digital filter is used, as depicted in Fig. 22, and the burden of the LPF that reduces the power of the folded spectrum can be reduced. In Fig. 22, the cutoff frequency of the analog LPF is actually set wide. Without a digital filter, the side lobe adjacent to the main lobe must be reduced by an analog LPF, which requires an LPF with a low cutoff frequency. Thus, there is a high possibility that the data of the main lobe is affected. The cutoff frequency can be widened when a digital filter is applied, so that the demodulation can be easily performed without damaging the signal of the main lobe, as compared to the case with a steep analog LPF having a low cutoff frequency.

In Fig. 23, it is confirmed that the BER performance of the proposed scheme does not change even if a digital filter is applied to the proposed scheme. This is because the proposed scheme extracts appropriate sample points as seen in Fig. 11, on the receiver side. If a steep analog filter is applied, the BER performance deteriorates owing to the signal distortion. Additionally, in the case of the Q-SSB modulation scheme of previous studies as indicated in (1), the BER performance at roll-off rate of zero deteriorates in not only the fading channel but also AWGN channel, owing to the effect of extra Hilbert components [6]. Therefore, it is a great advantage that the BER performance of the proposed scheme with a digital filter that functions as an ideal LPF filter does not deteriorate in AWGN channel environment.

Summarizing the simulation results in Section VI, the multiplexed SSB 4PAM with the digital filter has an ideal spectrum with a roll-off rate of zero, and the BER performance in the CNR is superior by 3 dB compared to the conventional DSB 16QAM, which has equivalent spectral efficiency. The advantage of the proposed scheme is that a spectrum with roll-off rate of zero can be generated without being affected by extra Hilbert components.

VII. Conclusion

In this study, 4ASK-based SSB modulation scheme with a digital filter is proposed. It has been confirmed that under AWGN channel environment the BER performance of the proposed scheme is superior by 3 dB in terms of the CNR to the 16QAM signal for the same data rate and the same occupied bandwidth, and maintains the good performance even in higher order modulation. Additionally, in terms of frequency efficiency, the proposed scheme realizes the ideal spectrum with the minimum required bandwidth without affecting the BER performance. Therefore, in the case of a single-carrier transmission, it is confirmed that the proposed ASK-based SSB modulation scheme is superior in the quality to DSB QAM scheme.

References

[1] H. Waraya and M. Muraguchi, “Proposal of a Quadrature SSB modulation Scheme for Wireless Communication Systems,” The Nineteenth International Conference on Networks (ICN2020), pp. 1-6, 2020.

[2] B. Pitakdumrongkija, H. Suzuki, S. Suyama, and K. Fukawa, “Single Sideband QPSK with Turbo Equalization for Mobile Communications,” 2005 IEEE 61st Vehicular Technology Conference, pp. 538-542, May 2005.

[3] Y. Jiang, Z. Zhou, M. Nanri, G. Ohta, and T. Sato, "Performance Evaluation of Four Orthogonal Single Sideband Elements Modulation Scheme in Multi-Carrier Transmission Systems," 2011 IEEE 74th Vehicular Technology Conference, pp. 1-6, September 2011.

[4] Y. Jiang, Z. Zhou, M. Nanri, G. Ohta, and T. Sato, "Inter-Signal Interference Cancellation Filter for Four-Element Single Sideband Modulation," 2012 75th Vehicular Technology Conference, pp. 1-5, 2012.

[5] A. M. Mustafa, Q. N. Nguyen, T. Sato, and G. Ohta, "Four Single-Sideband M-QAM Modulation using Soft Input Soft Output Equalizer over OFDM," The 28th International Telecommunication Networks and Applications Conference (ITANAC 2018), pp. 1-6, November 2018.

[6] B. Pitakdumrongkija, H. Suzuki, S. Suyama, and K. Fukawa, "Coded Single-Sideband QPSK and Its Turbo Detection for Mobile Communication Systems," IEEE Transactions on Vehicular Technology, VOL. 57, NO. 1, pp. 311-323, January 2008.

[7] X. Wang, M. Hanawa, and K. Nakamura, "Sideband Suppression Characteristics of Optical SSB Generation Filter with Sampled FBG Based 4-taps Optical Hilbert Transformer," 15th APCC, pp. 622-625, 2009.

[8] C. C. Tseng and S. C. Pei, "Design of discrete-time fractional Hilbert transformer," IEEE International Symposium on Circuits and Systems, pp. 525-528, May 2000.

[9] K. Takao, N. Hanzawa, S. Tanji, and K. Nakagawa, "Experimental Demonstration of Optically Phase-Shifted SSB Modulation with Fiber-Based Optical Hilbert Transformers," OFC/NEOEC, 2007.

[10] J. G. R. C. Gomes and A. Petraglia, "A switched-capacitor DSB to SSB converter using a recursive Hilbert transformer with sampling rate reduction," ISCAS 2000, pp. 315-318, 2000.

[11] S. A. Mujtaba, "A Novel Scheme for Transmitting QPSK as a Single-Sideband Signal," IEEE GLOBECOM 1998, pp. 592-597, 1998.